Document downloaded from:

http://hdl.handle.net/10251/154803

This paper must be cited as:

Puche Panadero, M.; Velty, A. (2019). Readily available Ti-beta as an efficient catalyst for greener and sustainable production of campholenic aldehyde. Catalysis Science & Technology. 9(16):4293-4303. https://doi.org/10.1039/c9cy00957d

The final publication is available at

https://doi.org/10.1039/c9cy00957d

Copyright The Royal Society of Chemistry

Additional Information

ARTICLE

Readily available Ti-Beta as efficient catalyst for greener and sustainable production of campholenic aldehyde

Received 00th January 20xx,
Accepted 00th January 20xx

DOI: 10.1039/x0xx00000x

Marta Puche Panadero and Alexandra Velty*

Different Ti-Beta zeolite samples were prepared following a convenient and optimized post-synthetic route and starting from commercial Al-Beta zeolite. Lewis acid sites has been successfully incorporated into the vacant tetrahedral (T)-sites of a dealuminated Beta-framework by ball-milling solid-state ion-exchange. A tribology-ball milling process was used in order to increase the interaction between dealuminated-Beta zeolite and Ti-precursor. Thermal treatments with water and aqueous solution of $NaNO_3$ or Li NO_3 allowed to optimize the catalytic properties of the Ti- Lewis active sites which exhibited excellent catalytic activity and stability for the isomerization of α-pinene oxide into campholenic aldehyde in both batch and fixed bed reactor systems. Additionally, the catalytic performance of post-synthesised Ti-Beta was compared to a Ti-beta prepared in fluoride media. From different point of views such as the preparation of readily, highly active, selective and stable catalyst, throughput, sustainability and cost, herein we report the selective solid catalysed α-PO isomerization with excellent results, 88% selectivity and yield, CA production of 225 $g/g_{cat}/h$ and new opportunities.

1. Introduction

In response to the needs of sustainable chemistry and the use of renewable feedstock, terpenes offer a large and versatile class of organic compound that are widely found in essential oils and are useful for fine chemicals industry. One of the most important source of terpenes is the turpentine oleoresin, extracted from coniferous trees whose main components are α- and β-pinene. Campholenic aldehyde (CA) is an important intermediate in the synthesis of several sandalwood fragrances and can be obtained through two-steps synthesis from α-pinene. In the first step the epoxide is obtained, being the α-pinene oxide isomerized, preferably in the presence of an acid catalyst, in a second step, providing different products of high-added value (Scheme 1). The isomerization has been widely studied in the last years in the presence of homogeneous and heterogeneous acid catalysts providing different products through competitive and consecutive reactions [1-3]. Several studies reported that Lewis acids favour the formation of campholenic, iso-campholenic aldehydes and trans-3-pinanone, while Brønsted acids result in the carveols and p-cymene. Selective preparation of campholenic aldehyde is conventionally catalysed by homogeneous Lewis acids such as $ZnCl_2$ and $ZnBr_2$ giving up to 85% yield of the desired aldehyde. However, there are numerous associated drawbacks such as a rapid deactivation of the catalysts or the production of large amount of contaminated waste with heavy metal due to the neutralisation step and the no opportunity of recycling [4-6]. Being numerous the advantages of the heterogeneous catalysts, different studies using solid Lewis acids have been reported. Likewise, Van Bekkum and co-workers reported the high catalytic performance of free Al Ti-beta zeolite to perform the isomerization of α-pinene oxide, with CA selectivity up to 89% in the liquid phase and up to 94% in the gas phase. Indeed, among nanoporous materials with higher surface areas, enhanced activity and providing shape/size selectivity, zeolites are clear candidates for this reaction. This is due to thermal stability, flexibility in their chemical composition with the possibility of accommodating different metals in its framework. An important breakthrough in the field of zeolites occurred with the synthesis of titanium silicalite (TS-1) [7], which was able to carry out the oxidation of different organic compounds with H_2O_2. However, TS-1 presents geometric limitations to react larger molecules. Then, the synthesis of large pores zeolites

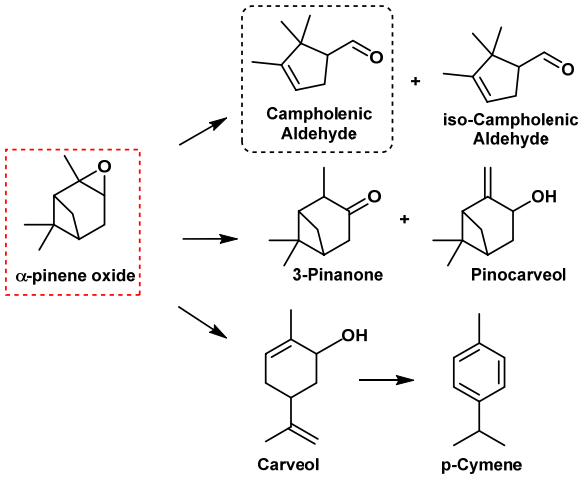

Scheme 1. Main products of isomerization of α-pinene oxide.

Instituto de Tecnología Química, Universitat Politècnica de València-Consejo Superior de Investigaciones Científicas, Avenida de los Naranjos s/n, E-46022 Valencia, Spain. E-mail: avelty@itq.upv.es, Tel: +34963879697.

† Footnotes relating to the title and/or authors should appear here.

Electronic Supplementary Information (ESI) available: [details of any supplementary information available should be included here]. See DOI: 10.1039/x0xx00000x

Please do not adjust margins

started with the preparation of Ti-Beta initially by-post synthesis treatment [8] and later by isomorphous substitution of Si with Ti by direct synthesis [9, 10]. Nevertheless, the catalytic properties of Ti-Beta were clearly worse than TS-1 and the differences were attributed to the presence of Al in the framework, to a high density of connectivity defects (Si-OH groups giving hydrophilic properties) and to a higher acidity of framework Ti species. Afterward, an unseeded method in fluoride medium to obtain zeolite completely free of Al and connectivity defects was developed improving definitively the catalytic properties of Ti-Beta [11]. Nevertheless, despite the advances and the academic interest, the synthesis of Ti-zeolites in fluoride medium sets out different drawbacks such as long crystallization time and the use of hazardous fluoride that causes technical and environmental problems of corrosion and pollution.

From this point, different alternative strategies can be followed to improve the methodology. For example the use of lower toxic source of fluoride such as ammonium or seeds in order to decrease synthesis time. Other post-synthesis methods have been developed involving the incorporation of metal (M^{IV} (Sn, Ti, Zr)) sites into the tetrahedral defects (sites) of modified beta zeolite framework. These routes start with the synthesis of Al or B beta zeolites, followed by the heteroatom removal and the creation of defects by acid treatments [12, 13]. Then, the silanol groups generated can be used for anchoring the M^{IV} precursors. Then different strategies were followed to introduce M^{IV} such as chemical vapor deposition, solid-state mixing (grinding) [16], grafting at solvent reflux [17], or wetness impregnation [18] with adequated M^{IV} containing reactants.

Another parameter of paramount importance is the presence of alkali ions. Indeed, the presence of high content of alkali ion during the synthesis of TS-1, Ti-Beta, and Sn-MFI constitutes an impediment to the crystallization of pure phase, precipitating metal oxide [19, 20]. Moreover, it was shown that alkali ions modify negatively the catalytic performance of zeolites for oxidation process [21, 22]. In contrary, other studies showed the positive effect of the addition of small amount of alkali ions such as for the epoxidation with H_2O_2 over TS-1, an increase of epoxide selectivity was observed and attributed to the neutralization of acid sites. Another experimental and computational work showed that the enhancement of catalytic performance for epoxidation could be attributed to weak cation-π interactions between heavy alkali metal cations and adjacent olefin molecules improving their diffusion within the micropores. In contrary, light alkali metal cations difficult the diffusion because of stronger cation-π interaction [23]. In this way, recent papers report the positive effect of the controlled presence of alkali ions in Sn-zeolites added in the reaction medium or for synthesis or post-synthesis treatment over their catalytic performance for sugars isomerization [24] and epimerization [25] or the conversion of sucrose into methyl lactate.

In this paper, we reported a convenient and optimized post-synthetic route for the preparation of Ti-Beta zeolite in where it has been successfully incorporated Lewis acid sites into the vacant tetrahedral (T)-sites of a dealuminated Beta-framework by ball-milling solid-state ion-exchange. A tribology-ball milling process was used in order to increase the interaction between dealuminated-Beta zeolite and Ti-precursor. Then, after consecutive processes of thermal treatment and calcination thanks to reversible hydrolysis of Ti-O-Si bonds and condensation steps we modified the coordination and so the nature of Lewis acid Ti centres. Moreover, partial cation exchange with alkali metal allowed to match the catalytic properties of Ti-Beta. Therefore, following this procedure it is possible to prepare optimized Ti-beta catalyst where Ti was tetrahedrally coordinated within the zeolite framework, with excellent activity as Lewis acid catalyst and stability for the isomerization of α-pinene oxide into campholenic aldehyde in both batch and fixed bed reactor systems. Additionally, the catalytic performance of post-synthesised Ti-Beta was compared to a Ti-beta prepared in fluoride media.

2. Results and discussion

2.1 Catalysts characterisation

The preparation of Ti-Beta post-synthesis zeolite (Ti-Beta-PS) started by dealumination of a readily available commercial Al-Beta zeolite (Si/Al= 13) with an treatment in aqueous solution of HNO_3 (see experimental). The ICP analysis demonstrated that Al was removed from the original material (Table 1) and the XRD pattern showed no structural changes in the Beta zeolite sample (Figure S1). From FT-IR spectroscopy it was seen that Al-Beta zeolite exhibited two characteristic bands of Brønsted acid sites (BAS) at 3610 cm^{-1} due to the presence of proton as cation of compensation of the negative charge associated to Al (Si–O(H)–Al), and isolated silanol groups at 3740 cm^{-1} (Figure S2). The FT-IR spectra of dealuminated Beta zeolite sample only registered the band at 3740 cm^{-1} supporting the removal of Al tetrahedrally coordinated. In a second step, the Ti atoms were incorporated in the vacant through solid state ion exchange by ball milling of dealuminated zeolite and Cp_2TiCl_2 (see experimental). After calcination at 550 ºC in order to remove organic species and to complete the incorporation of Ti into the Beta zeolite framework, the DRUV-Vis spectrum obtained for Ti-Beta-PS sample shows broad and poorly defined absorption band in the 205-220 nm region that could indicate the formation of multiple metal species (Figure S3). Nevertheless, no indication of absorbance at 330-350 nm was observed, suggesting low presence of TiO_2 octahedrally coordinated. Moreover, the plotted UV-Vis spectrum seem similar to those reported [26]. These data allow to conclude

Table 1. ICP analysis of post-synthesised Ti-Beta samples and DeAl-Beta.

Samples	Li%	Na%	Ti%	Si%	Al%	Si/Al	Si/Ti
deAl-Beta	-	-	-	41.06	0.02	1972	-
Ti-Beta-PS	-	-	1.68	44.56	0.02	2675	45
Ti-Beta-PS-HT	-	-	1.71	40.49	0.015	2778	40
Ti-Beta-PS-HT-Na	-	0.1	1.68	44.57	0.02	2676	45
Ti-Beta-PS-HT-Li	0.04	-	1.89	45.74	0.02	2585	41

This journal is © The Royal Society of Chemistry 20xx

Please do not adjust margins

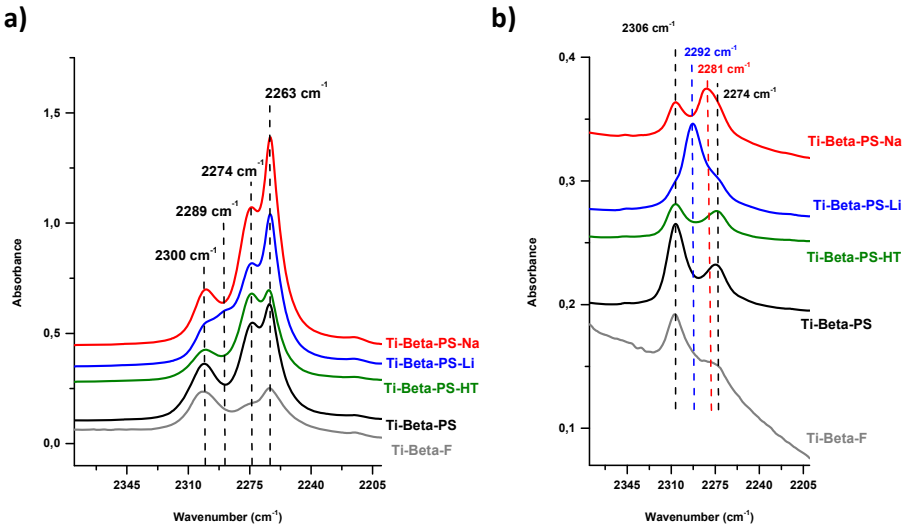

Figure 1. CD_3CN adsorption/desorption profile for the different Ti-Beta-PS samples, (a) maximum coverage and (b) after desorption for 4 minutes.

that prepared sample contained isolated metal species and tetrahedrally coordinated within the zeolitic framework, and probably no bulk oxides. Finally, the preservation of crystallinity after the steps of dealumination and ball-milling for the incorporation of Ti was confirmed from the XRD (Figure S4).

In order to study the effect of the presence of alkali ions over the catalytic performance of Ti-Beta zeolite, we prepared exchanged Na and Li Ti-Beta-PS samples. For this, Ti-Beta-PS sample was treated with aqueous solution of $LiNO_3$ and $NaNO_3$ at 80ºC for 15h (see experimental). After calcination, similar DRUV-Vis spectra obtained for Ti-Beta-PS were registered with Ti-Beta-PS-HT, Na and Li samples show absorption in the 205-220 nm ultraviolet region that could indicate the formation of isolated metal species while the no indication of absorbance at 330-350 nm suggested the absence of TiO_2 (Figure S3). ICP analysis (Table 1) confirms the presence of Na and Li in the treated samples as well as that Ti wt% content remained constant. More especially, Li and Na content was of 0.04% and 0.1% respectively, i.e a 13 and 10 mol% respect to Ti, respectively.

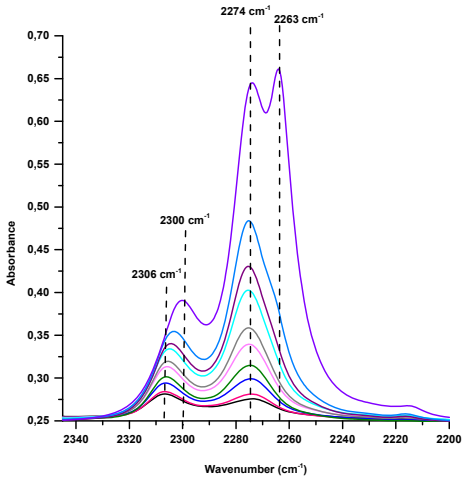

Figure 2. In situ CD_3CN desorption profile for Ti-Beta-PS-HT. CD_3CN was desorbed under a dynamic vacuum at room temperature.

To obtain more information about of titanium speciation within Ti-Beta-PS samples as synthesised and after thermal treatment with $NaNO_3$, $LiNO_3$, FT-IR CD_3CN absorption was performed. When deuterated acetonitrile was adsorbed on the different calcined Ti-Beta samples, several bands in the 2260–2310 cm^{-1} IR region associated with ν(C≡N) stretching vibration were observed. The adsorption band at ±2263 cm^{-1} corresponds to weakly physisorbed CD_3CN and disappeared at the maximum of desorption (Figure 1b). There was a noticeable shoulder at ±2274 cm^{-1} that was attributed to CD_3CN coordinated to Brønsted acid sites likely due to the silanol species that were present in the materials. Following desorption under dynamic vacuum for various time periods, it is clear that the weakly-bound physisorbed CD_3CN was first removed, followed by the CD_3CN species bound to the Brønsted acid sites (Figure 2). The presence of silanol groups was supported by the FTIR spectra of activated Ti-Beta zeolites in the OH stretching region. Indeed, it was observed that post-synthesis samples present a large number of silanol groups as it could be expected due to the methodology of the procedure since the dealumination as well as the incorporation of Ti atoms via a solid state ion-exchange by ball milling induced silicon coordination defect. Then the two bands at ±3736 and ±3746 cm^{-1} were assigned to terminal Si-OH groups (Figure 3). The difference in wavenumbers was primarily related to the silanol groups being involved or not in weak hydrogen bonding. Thus, the band at ±3743 cm^{-1} was assigned to free Si-OH groups [27], at ±3736 cm^{-1} being assigned to those Si-OH groups in which the O is weakly hydrogen bonded to an adjacent OH moiety [28]. These acidic Si-OH groups were partially or totally passivated by post-synthesis modification with alkali cations. From both spectra, it is concluded that post-

Please do not adjust margins

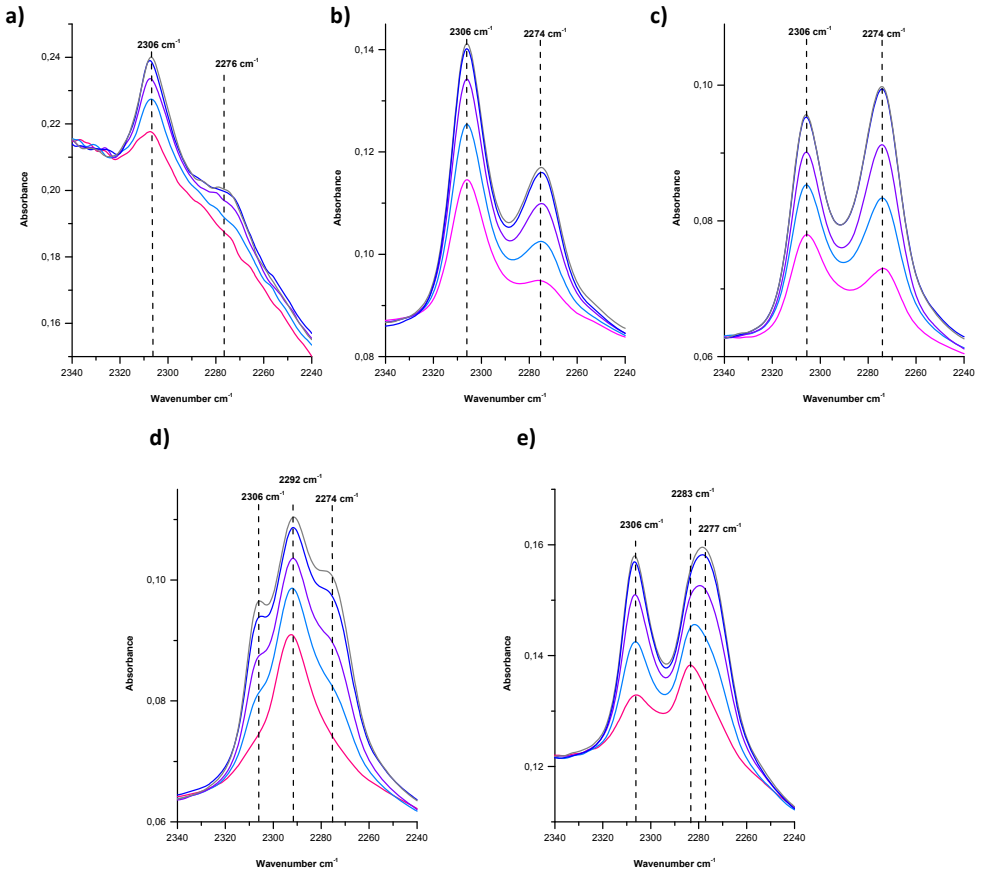

Figure 3. IR spectra at increasing acetonitrile coverage (1.9 mBar), on (a) Ti-Beta-PS, (b) Ti-Beta-PS-HT, (c) Ti-Beta-PS-HT-Na, (d) Ti-Beta-PS-HT-Li and (e) Ti-Beta-F samples.

synthesised Ti-Beta samples present a larger density of silanol groups than Ti-Beta synthesised in fluoride media practically without defect of coordination.

CD_3CN adsorption bands at ±2306 and ±2300cm^{-1} were also observed and corresponds to coordinated CD_3CN onto the Ti^{IV} Lewis acid centres [20]. Considering the IR spectra at increasing acetonitrile low coverage over the different samples, initially CD_3CN adsorption band at ±2306 cm^{-1} (Figure 3) and at higher coverage CD_3CN adsorption band at ±2300 cm^{-1} were observed (Figure 1 (a) and Figure S5). Therefore, if we take into accounts studies of IR CD_3CN absorption on Sn-Beta [29] and by analogy we assume that the fact that there are two bands indicate that two types of Lewis acids sites (LAS) are present. Moreover, the higher relative shift of the band and the fact that the adsorption initiates at 2306 cm^{-1}, allow to suggest that Lewis acid sites at 2306 cm^{-1} interacts more strongly with acetonitrile than the other at 2300 cm^{-1}. Indeed, in the case of Sn-Beta, partially

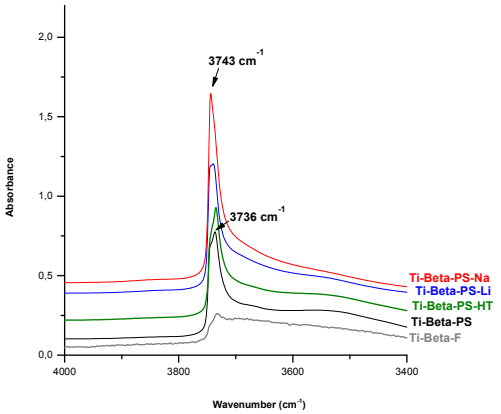

Figure 4. IR spectra in the OH stretching region for the different Ti-Beta-PS samples after activation.

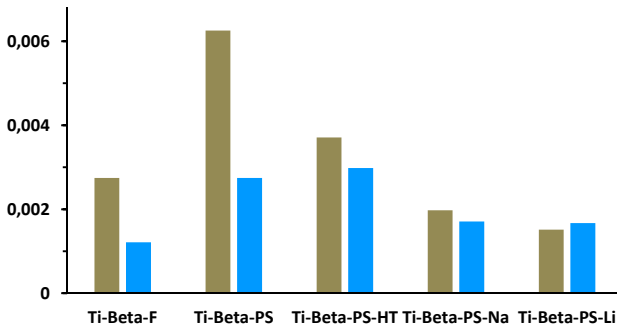

Figure 5. Comparison after normalisation (sample weight) of the CD_3CN absorbance on Ti-Lewis acid site at (▪) 2308cm^{-1} and weak Brønsted acid SiO-H groups at (▪) 2274 cm^{-1}.

This journal is © The Royal Society of Chemistry 20xx

Please do not adjust margins

Table 2. Effect of metal Lewis acid centre.

Catalyst	Conv. α-PO%	CA Sel.%	TON*	Yield %				
				CA	3-Pinanone	Iso-CA	Carveol	Pinocarveol
deAl-Beta	28.1	47.4	-	13.3	0.8	1.9	3.0	1.2
Ti(1.9%)-Beta-F	93.7	82.1	3718	76.9	1.8	2.3	3.2	0.1
Ti(1.7%)-Beta-PS	95.3	59.8	3248	57.0	4.0	5.4	8.5	0.4
Zr(1.9%)-Beta-F	93.1	26.3	2281	24.5	28.0	13.1	9.2	0.6
Sn(1.9%)-Beta-F	99.1	17.3	2050	17.2	29.6	29.0	7.9	0.3

Reaction conditions: Reaction conditions: microwave heating, 150ºC, 25mg of zeolite, 2 mmol of α-PO, 760 mg of acetonitrile and 3 min of reaction time.*TON was calculated as the number of moles of CA produced by the number of mole of metal as active sites.

hydrolysed and nonhydrolysed framework Sn sites, or open-closed sites, were identified and attributed to adsorption bands at ±2308 and ±2316 cm^{-1}, respectively. In the case of titanosilicates, reported detailed EXAFS studies of TS-1 allowed to distinguish between the tetrapodal and tripodal ($Ti(OSi)_3OH$) structures [30]. Similarly, the bands at ±2300 and ±2306cm^{-1} are assigned to open-closed Ti-Lewis acid centres.

Additionally, for Ti-Beta-PS-HT-Li a new band at ±2292 cm^{-1} is detected (Figure 1 and Figure 3 (d)). In comparison to IR spectra of CD_3CN on Sn-Beta-Li reported by Tatsumi and co-workers [31] this band is assigned to CD_3CN adsorption on Li cations that can act as Lewis acid sites. When we compare the minimum acetonitrile coverage spectra of the five Ti-Beta samples (Figure 3 a, b, c, d and e, Figure 4) it is noticeable that Ti-Beta-F and Ti-Beta-PS samples present different density of Lewis acid sites and of silanol groups. This tendency is illustrated in Figure 5 where after normalization (wafer weight of zeolite sample), CD_3CN absorbance heights at ±2306 and ±2274 cm^{-1} determined after deconvolution of the IR spectra with the ORIGIN software program (Figure S6) were plotted. It is clear that Ti-Beta-PS sample presents a higher number of strong Ti-Lewis acid sites than other Ti-Beta samples and that through post synthesis thermal treatment and cation exchange the population of strong Ti-Lewis acid sites (Ti-LAS) and of silanol groups were modified and decreased. In the case of Ti-Beta-PS-Li sample, the CD_3CN adsorption over Li induces an overlapping of the band at ±2292 cm^{-1} together with the band at 2306 cm^{-1} (Figure 1 (b) and Figure S6 (b)). The lower shift of the bands indicates that Li can acts as weaker Lewis acid sites than Ti, while the changes in the intensity of the band at ±2306 cm^{-1} indicates a weakening of Ti-Lewis acid sites respect to IR CD_3CN spectra of Ti-Beta-PS and Ti-Beta-PS samples. Tatsumi and co-workers showed that the weakening of Sn-Lewis acid sites was enhanced by increasing the size of the cations from Li to Cs, and that the more adequate cation to maintain the original Lewis acidity on the Sn atoms was Li. Different works reported that the incorporation of alkali metal occurred through cation exchange with proton of SiO-H close to Sn and not on SnO-H [25, 31]. Moreover, that cation exchange takes place indifferently on both closed and open Sn sites through dynamic hydrolysis of Si–O–Sn bonds during aqueous treatment. In the case of Ti-Beta-PS-HT-Na a new band at ±2282 cm^{-1} is detected indicating that adsorption on Na was weaker than on Li (Figure 1 and Figure 3 (c)) while both bands at ±2306 and ±2300 cm^{-1} were maintained, indicating that Lewis acidity of Ti-atoms was preserved.

These data of characterisation showed that with a small amount of Li or Na, partial cation exchange on SiO-H close to Ti atoms occurred, passivating Brønsted acidity of adjacent silanol groups and maintaining the Lewis acidity of Ti-atoms similarly to what was described with Sn-Beta zeolites but modifying both density of Ti-Lewis acid and weak Brønsted acid sites.

2.2 Catalytic activity tests

Reaction in sealed vial under microwave

At first, the catalytic tests of the titanosilicate catalysts herein prepared for the α-pinene oxide isomerization were performed in sealed vial under microwave irradiation. The benefits of microwave heating over conventional ovens are well known, such as higher rate of reaction, better yield and higher selectivity (less formation of side product), high reproducibility thanks to the homogeneity of microwave irradiation and finally a lower energy usage. In Table 2, the catalytic activity of different Beta samples prepared conventionally in fluoride medium and incorporating different metal with Lewis acid properties such as Ti, Sn and Zr were compared. Because of the high reactivity of α-pinene oxide different isomerization products were formed and detected such as carveols, iso-campholenic aldehyde, 3-pinanone and pinocarveol (Scheme 1). As it has been reported in the bibliography, the more adequate metal

Table 3. Effect of hydrothermal treatment over the catalytic performance of post-synthesized Ti-beta.

Entry	Catalyst	Conv.%	Yield %					CA Sel. %
			CA	3-Pinanone	Iso CA	Pinocarveol	Carveol	
1	Ti-Beta-F	93.7	76.9	1.8	2.3	0.1	3.2	82.1
2	Ti-Beta-PS	95.3	57.0	4.0	5.4	0.4	8.5	59.8
3	Ti-Beta-PS-HT	97.2	79.9	1.9	1.9	0.2	3.8	82.2
4	Ti-Beta-PS-HT-Li(0.04%)	99.1	86.5	1.5	1.4	0.1	2.6	87.3
5	Ti-Beta-PS-HT-Na(0.1%)	97.1	83.3	1.5	1.3	0.6	2.5	85.8

Reaction conditions: Reaction conditions: microwave heating, 150ºC, 25mg of zeolite, 2 mmol of α-PO, 760 mg of acetonitrile and 3 min of reaction time.

Please do not adjust margins

Table 4. Effect of addition $NaNO_3$ or $LiNO_3$ following different method.

Entry	Catalyst	α-PO Conv.%	Yield%			CA Sel.%	Cation %	Method
			CA	Pinanone	Iso-CA			
1	Ti(1.9%)-Beta-PS-HT	95.6	81.6	2.7	2.5	85.3	0.00%	-
2	Ti(1.9%)-Beta-PS-Li(0.04%)	99.8	88.6	2.4	2.3	88.8	0.04%	Li-reflux
3	Ti-Beta-PS-HT-Li-1	93.9	77.4	1.8	1.9	82.4	0.01%	Li-impregnation
	Ti-Beta-PS-HT-Li-2	86.3	72.5	2.1	1.9	84.0	0.03%	Li-impregnation
4	Ti-Beta-PS-HT-Li-3	84.8	70.9	2.0	1.7	83.7	0.06%	Li-impregnation
5	Ti-Beta-PS-HT-Li-4	93.5	77.1%	2.3	2.1	82.5	0.03%	Li-solution
6	Ti-Beta-PS-HT-Na(0.04%)	99.2	83.6%	2.4	2.3	84.3	0.04%	Na-reflux
7	Ti-Beta-PS-HT-Na-1	96.7	83.2%	2.0	2.1	86.1	0.02%	Na-impregnation

Reaction conditions: microwave heating, 150ºC, 8 mg of zeolite, 2 mmol of α -PO, 380 mg of acetonitrile and 8 min of reaction time.

to perform the isomerization of α-PO was Ti. Under the reactions conditions, CA was obtained with yield and selectivity up to 76.9 and 82.1%, after 3 min of reaction time and the calculated TONs allowed to order the catalytic performance of the different metal-zeolite samples to produce CA as follows: Ti-Beta-F>Ti-Beta-PS>Zr-Beta-F>Sn-Beta-F (Table 2). As we mentioned above the preparation Beta samples incorporating Ti, Zr or Sn in fluoride media involves several drawbacks and so pushed to research and develop alternative routes of synthesis. Likewise we studied the preparation of Ti-Beta zeolite following a post-synthesis method based on the dealumination of Al-beta commercial sample and the posterior incorporation of Ti in the tetrahedral defects generated through solid state ion-exchange process using a ball-mill. It has been reported than only tetrahedrally and 5-coordinated Ti species acted as Lewis acid active sites and that extra-framework species with octahedral coordination were inactive species [32, 33]. From characterisation data we showed the successful incorporation of Ti in tetrahedrally coordinated position. In Table 3, the results obtained over the different Ti-beta samples following conventional method in fluoride medium and, following a post-synthesis method are reported. The results of Table 3, Entries 1 and 2 showed that Ti-Beta-PS exhibited notably lower selectivity to CA than Ti-Beta-F. Additionally, the catalytic performance of the dealuminated Beta sample (deAl-Beta) was explored. As it could be expected, deAl-Beta exhibited low catalytic activity and CA selectivity. Considering the route of preparation of the Ti-Beta-PS sample and the IR characterisation data, this result was attributed to the coordination defects created during the incorporation of Ti into the Beta framework and so to the presence of high density of silanol groups with weak Brønsted acidity, providing distinct active centres that exhibit diverse activity and selectivity. In order to improve the catalytic performance of the Ti-Beta sample, we envisioned that consecutive processes of thermal treatment and calcination thanks to reversible hydrolysis of Ti-O-Si bonds and condensation steps could modify the coordination and so the nature of Lewis acid Ti centres (partially hydrolysed and nonhydrolysed). As well as, a study of cation exchange with alkali metal can allow us to match the catalytic properties of Ti-Beta inhibiting the weak Brønsted acidity of adjacent silanol groups to Ti-atoms on the one hand and adjust the Ti-Lewis acid strength on the other hand. For this, Ti-Beta-PS was treated with different aqueous solutions of $LiNO_3$, $NaNO_3$ and water at 85ºC for 15h. After calcination, the catalytic performance exhibited by the three Ti-Beta-PS samples submitted to hydrothermal treatment were notably improved (Table 3, entries 3-5). Interestingly, after a simple hydrothermal treatment at 85ºC and calcination, the catalytic performance of Ti-Beta-PS was considerably improved since the CA selectivity increased from 59.8 up to 82.2 %. This catalytic results were similar to ones achieved in the presence of Ti-Beta-F. From Figure 5, it was noticeable that Ti-Beta-PS presented the highest density of strong Lewis acid sites as well as of weak Brønsted acid sites (SiO-H) (BAS). However, after hydrothermal treatment Ti-Beta-PS-HT has lower density of Ti-LAS than Ti-Beta-PS but similar to Ti-Beta-F, while the density of BAS are similar for both samples Ti-Beta-PS and Ti-Beta-PS-HT and higher than Ti-Beta-F. When the Ti-Beta-PS catalytic behaviour was checked after the hydrothermal treatment, with $NaNO_3$ and $LiNO_3$ solutions and calcination steps, the results showed that it is possible to increase newly the CA selectivity up to 87.3 %. Now, the achieved CA selectivity is higher than one exhibited in the presence of Ti-Beta-F.

Table 5. Effect of nature of solvent over the catalytic performance of post-synthesized **Ti-Beta-PS-HT-Na(0.1%).**

Solvent	Conv. α-PO%	CA Sel.%	Yield %				
			CA	3-Pinanone	Iso-CA	Carveol	Pinocarveol
ACN	93.2%	83.4%	77.8%	2.4%	2.1%	2.7%	0.5%
Toluene	87.0%	86.2%	75.0%	5.3%	2.9%	1.8%	0.1%
DMA	9.4%	78.9%	7.4%	0.4%	0.7%	1.5%	0.2%
MeCyHex.	83.5%	78.7%	65.7%	4.3%	2.7%	2.1%	0.9%

Reaction conditions: Reaction conditions: microwave heating, 150ºC, 8 mg of zeolite, 2 mmol of α-PO, 0.485 mL of solvent and 8 min of reaction time.

This journal is © The Royal Society of Chemistry 20xx

Please do not adjust margins

Additionally the CA selectivity, α-PO conversion and kinetic constant were plotted versus the height of Lewis acid sites at 2306 cm^{-1} and Brønsted acid sites at 2274 cm^{-1}. The Figure S7 illustrates that a correlation between the height of Lewis acid sites and CA selectivity and kinetic constant was established, decreasing the CA selectivity as well as kinetic constant with an increase of the height (number of Lewis active sites). Nevertheless, when the CA selectivity and kinetic constant were plotted versus the height of Brønsted acid sites no trend could be established. These results showed that the strength and number of Lewis active is a key factor to maximise the CA selectivity since the Li and Na cation exchange induced and a weakening in the Ti-Lewis acidity maximising CA selectivity. In the meantime, α-PO conversion remained constant regardless of the height of Lewis acid sites or Brønsted acid sites.

IR study of CD_3CN adsorption allowed to conclude that Li and Na cation were exchanged by proton of SiO-H group adjacent to Ti atom, partially hydrolysed or nonhydrolysed since treatment was performed in presence of water and that hydrolysis of Si-O-Ti occurred. In this way, the weak Brønsted acidity of silanol groups can be controlled and partially inhibited. Moreover, the alkali cation (Li and Na) not only exhibit Lewis-acidity but also induced a weakening in the Ti-Lewis acidity. These catalytic results showed that the catalytic properties of Ti-Beta-PS were modified through alkali cations exchange reducing side reactions and maximising α-PO conversion and CA selectivity. Then characterisation data together with catalytic performance of the different Ti-Beta samples let to conclude that Ti-Lewis acid strength was softened and tailored thank to the Li or Na cation exchange and the weak Brønsted acidity of Ti atoms adjacent SiO-H was passivated, maximising the catalytic properties of Ti-Beta sample to the production of CA.

In order to determine if there exist a maximum in the Na and Li content, a study of addition of Li and Na following different procedures was performed, by impregnation or by adding the alkali in solution in methanol (Table 4), either to the Ti-Beta catalyst or added directly to the reaction medium. The results were compared to hydrothermal treatment (Reflux). The addition of Li by impregnation or in methanol solution did not improved the catalytic performance of the Ti-Beta-PS-HT obtained by post-synthesis method and submitted to hydrothermal treatment at 85ºC for 15h, and on the contrary, we could observe a slight decrease of the catalytic results (Table 4, Entries 2-5). In the case of Na, a slight increase of the catalytic activity of the Ti-Beta samples was observed (Table 4, Entries 6 and 7).

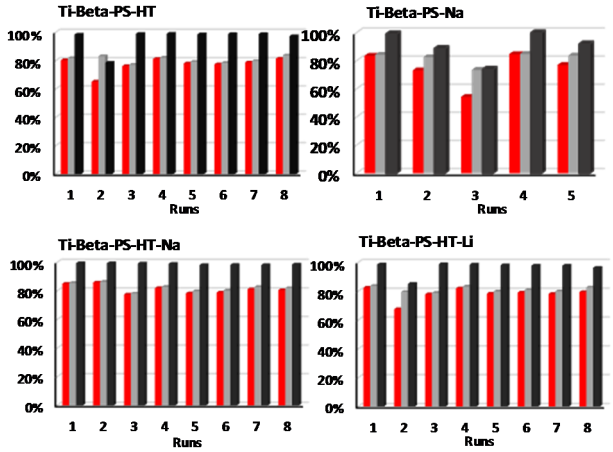

Figure 6. Reaction conditions: Reaction conditions: microwave heating, 150ºC, 8mg of zeolite, 2 mmol of α-PO, 380 mg of acetonitrile and 8 min of reaction time. ● CA yield, ● CA selectivity, ● α-PO conversion.

Then the stability of the catalytic activity of the different Ti-Beta samples was studied. For this purpose, different Ti-Beta catalysts were reused up to 8 consecutive runs. After each cycle, the solid catalyst was separated by filtration, washed with acetonitrile and calcined in air at 550ºC. Figure 6 showed that the different samples exhibited a stable catalytic behaviour along the different runs and that exchanged-alkali metal samples exhibited higher catalytic performance than Ti-Beta-HT. Noticeably, these results demonstrated that alkali metal was strongly exchanged and stabilized. In terms of yield and selectivity, Ti-Beta-PS-HT-Na(0.1%) exhibited slightly higher performance. So, we considered that Ti-Beta-PS-Na(0.1%) exhibited the more adequate catalytic properties.

In order to consider the nature of Ti active sites of the used catalysts, FT-IR CD_3CN absorption of the used Ti-Beta-PS-HT, Ti-Beta-PS-HT-Na and Ti-Beta-PS-HT-Li beta samples, after calcination at 550ºC for 5h, was performed. For both adsorption and desorption profiles of the used Ti-Beta-PS-HT, Ti-Beta-PS-HT-Na and Ti-Beta-PS-HT-Li samples, the same characteristic bands described for the original samples are observed. For adsorption (Figure S8 (a)), the band at ±2263 cm^{-1} corresponding to weakly physisorbed CD_3CN is lower for all post-synthesised samples respect to original ones. A shoulder at ±2274 cm^{-1} attributed to CD_3CN coordinated to Brønsted acid sites due to the presence of the silanol species as well as the band at 2300 cm^{-1} corresponding to coordinated CD_3CN onto the Ti^{IV} Lewis acid centres

Table 6. Effect of α-PO concentration over the catalytic performance of post-synthesized **Ti-Beta-PS-HT-Na(0.1%)**.

Entry	α-PO wt%	α -PO mol/L	Conv. α -PO%	CA Sel.%	Yield %				
					CA	3-Pinanone	Iso-CA	Carveol	Pinocarveol
1	54.5	5.7	93.0	84.9	79.0	2.5	2.1	2.7	0.5
2	47.8	4.1	93.2	83.4	77.8	2.4	2.1	2.7	0.5
3	30.2	2.1	98.2	87.3	85.8	2.2	1.9	2.7	0.4
4	18.2	1.0	96.0	89.0	85.5	1.9	1.6	1.9	0.1

Reaction conditions: microwave heating, 150ºC, 8 mg of Ti-Beta-PS-HT-Na(0.1%), 2 mmol of α -PO, different volume of acetonitrile. Ti content: 2 wt%.

Please do not adjust margins

Table 7. Effect of catalyst amount over the catalytic performance of post-synthesized **Ti-Beta-PS-HT-Na(0.1%)**.

Time (min)	wt%	Conv. α-PO%	CA Sel.%	Yield %				
				CA	3-Pinanone	Iso-CA	Carveol	Pinocarveol
12	1.2	71.9	82.2	59.1	2.1	1.8	2.4	0.6
8	2.3	93.2	83.4	77.8	2.4	2.1	2.7	0.5
4	3.4	93.4	85.1	79.5	2.2	1.9	2.6	0.4
3	5.1	99.4	84.8	84.2	2.3	2.0	2.8	0.4
2	7.0	99.4	86.3	85.7	2.2	1.9	2.8	0.4

Reaction conditions: Reaction conditions: microwave heating, 4, 8, 12, 18 or 25 mg of Ti-Beta-PS-HT-Na(0.1%), 2 mmol of α-PO, 375 mg of acetonitrile.

are present similarly to original samples. At maximum desorption (Figure S8 (b)), similar profiles are observed for Ti-Beta-PS-HT and Ti-Beta-F samples with two bands at 2308 and 2274 cm^{-1} corresponding to closed Ti-Lewis acid centres and Brønsted acid sites, respectively. Additionally, for Ti-Beta-PS-HT-Li the band at ±2292 cm^{-1} is detected. Different intensities of the different bands are observed, for the Ti-Beta-PS-HT-Li sample before and after reaction, indicating a subtle variation in the nature of the Lewis acid centers that nevertheless did not influence the catalytic activity of the sample since it can be reused without loss of selectivity or conversion (Figure 6). A similar subtle change in the bands intensity of the Ti-Beta-PS-HT-Na sample was observed at 2308 and 2281 cm^{-1}. Also in this case the slight changes in the nature of the Lewis acid active sites did not affect the catalytic properties of the Ti-Beta-PS-HT-Na sample that could be reused several cycles without loss of selectivity or conversion. DRUV-Vis spectra obtained for Ti-Beta samples after their use as isomerization catalyst were similar to ones registered for fresh catalysts (Figure S9). A broad and poorly defined absorption band in the 205-220 nm region indicates the formation of multiple metal species and no indication of absorbance at 330-350 nm suggests low presence of TiO_2 octahedrally coordinated. Then, the characterisation data of used Ti-Beta-PS samples allowed to confirm the stability of the active acid sites.

In chemical processes, it is important to select the optimum reactions conditions such as solvent (nature and amount) and temperature. More especially, in the case of solid catalysts where compete the co-adsorption/desorption of solvent, reactant and products. Competitive adsorption/desorption determine the intra-porous concentration of reactant and products and can modify greatly the process selectivity and side reaction productions. In the case of α-PO isomerization, different works reported the effect of polarity and basicity of the chosen solvents over the selectivity of the process [1-3]. As well as, non-polar solvent seemed to favour selective campholenic aldehyde while polar and basic solvents such as N,N-dimethylacetamide (DMA) allowed to increase the selectivity to carveols. Furthermore, in the case of Ti-Beta zeolite the synthesis procedure affects hydrophobic/hydrophilic properties of Ti-Beta controlled by the density of silanol groups. A sample without defects, i.e. with a reduced amount of silanol groups, will preferentially adsorb non-polar molecules over more polar ones. Thus, the catalytic results of the use of 4 different solvents were reported in the Table 5 using Ti-Beta-PS-HT-Na(0.1%) as catalyst. We observed that at 150ºC the Ti-Beta-PS sample herein prepared was totally deactivated by the use of DMA, due to strong adsorption over active sites, being the conversion only of 9.4%. The result was in disagreement with recently published paper where the use of DMA for α-PO isomerization in the presence of Ti-MWW produced at 140ºC CA with selectivity close to 75% at 75% conversion of α-PO. In the case of Ti-Beta-PS-HT-Na(0.1%) the best selectivity were obtained with acetonitrile and toluene, up to 86%, being higher the conversion in the presence of acetonitirile (93%) which appears more suitable solvent.

Given that for the development of greener process and the improvement of throughput, it is of great importance to limit the use of solvent. With this purpose, a series of experiments varying α-PO concentration in the reaction medium were carried out. As it could be expected a maximum selectivity of 89 % was achieved with lower α-PO concentration (Table 6). Additionally, the results of Table 7

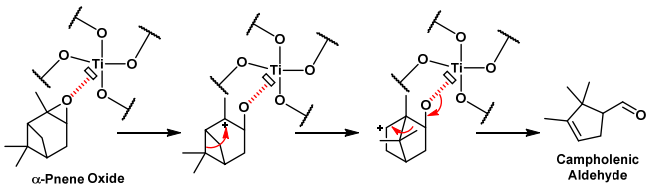

Scheme 2. Proposed mechanism for the isomerisation of α-PO

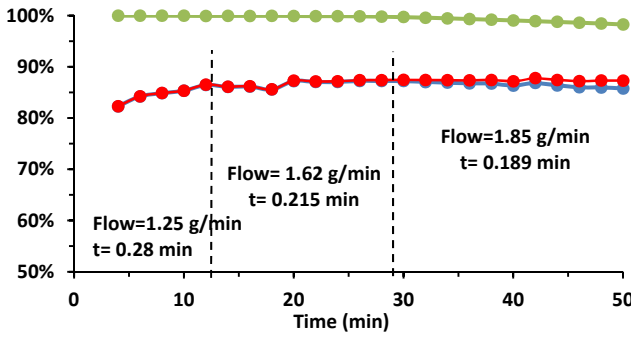

Figure 7. Effect of contact time over α-PO conversion and CA yield and selectivity in fixed bed. Reaction conditions: 450 mg of catalyst (0.2<particle size<0.4mm), 150ºC, 2 mmol of α-PO per 380 mg of acetonitrile, different contact time from 0.28 min to 0.189 min, i.e. total flow from 4.05 to 6 mL/min. ● CA yield, ● CA selectivity, ● α-PO conversion.

This journal is © The Royal Society of Chemistry 20xx

Please do not adjust margins

Please do not adjust margins

showed that a decrease of catalyst amount did not practically affect the CA selectivity and adjusting reaction time it was possible to produce CA with high yield and selectivity.

We believe that the ability of the post-synthesised Ti-Beta-PS-HT-Na(0.1%) sample from readily available Al-Beta, whose catalytic performance for the isomerization of α-PO was improved thanks to the Na-exchange was shown. The excellent catalytic performance of Ti-Beta-PS-HT-Na(0.1%) was due to the presence of tetrahedrally coordinated Ti sites in the silica-Beta framework whose Lewis acidity was matched through controlled hydrothermal incorporation of alkali-metal, with no Brønsted acidity. A proposed-mechanism of α-PO isomerization by Lewis acid was reported some time ago (Scheme 2) [2].

We think that in the developed reaction conditions, α-PO concentration and catalyst amount, present unprecedentedly catalytic results in terms of CA production and selectivity. Likewise, in order to take a step forward in the development of a process and a catalyst validated at laboratory scale on an industrial scale, all these results were transferred to a study in flow. Moreover, the implementation of continuous process will contribute to sustainability and greenness.

Reaction in fixed bed

Since parameters of reaction are key factors to optimize process performance space velocity, temperature and solvent were optimized in fixed bed. The first experiments performed at 150ºC with different space velocity from 1.25 to 1.85g/min per 0.45g of Ti-Beta-PS-HT-Na. The data of conversion, yield and selectivity plotted in Figure 7 reflected that high CA yield and selectivity can be achieved up to 87% at complete conversion. Figure 8 illustrates the effect of temperature over α-PO conversion and CA selectivity. The results proved that adsorption was affected strongly by temperature, since at 130ºC a constant decrease of conversion was observed from 98 to 86% and an increase of temperature until to 140 ºC allowed recovering maximum conversion of 99 % with CA selectivity close to 88%. This result showed that deactivation of the catalyst by adsorption of reagent and product was a reversible process and possible by a slight increase of temperature. To continue the temperature was increased until 150ºC and 160ºC, and really no drastic change over process selectivity was observed being around 87-86%. Since temperature has a slight effect over process selectivity, 140ºC was determined as more adequate temperature. As we proceeded in batch reactor, the isomerization was set up using different solvents, feeding successively α-PO solution in ACN, toluene, DMA and newly CAN (Figure 9). The results showed as in batch reactor that in the presence of DMA, the catalyst suffered a strong deactivation by adsorption of the solvent over the catalyst surface and metal active sites. Moreover, it was confirmed that is a

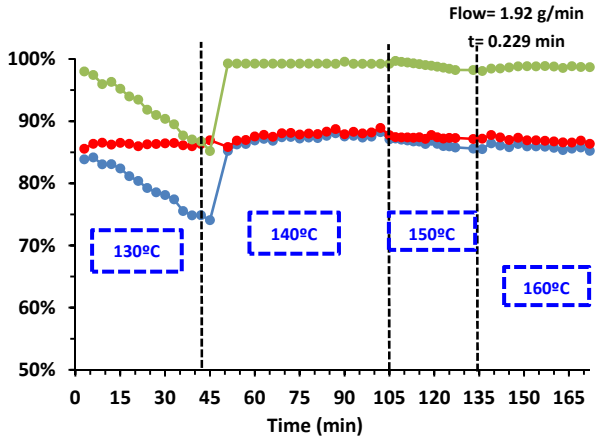

Figure 8. Effect of temperature over α-PO conversion and CA yield and selectivity in fixed bed. Reaction conditions: 450 mg of catalyst (0.2<particle size<0.4mm), 2 mmol of α-PO per 380 mg of acetonitrile, contact time from 0.229 min, i.e. total flow from 5.28 mL/min. ● CA yield, ● CA selectivity, ● α-PO conversion.

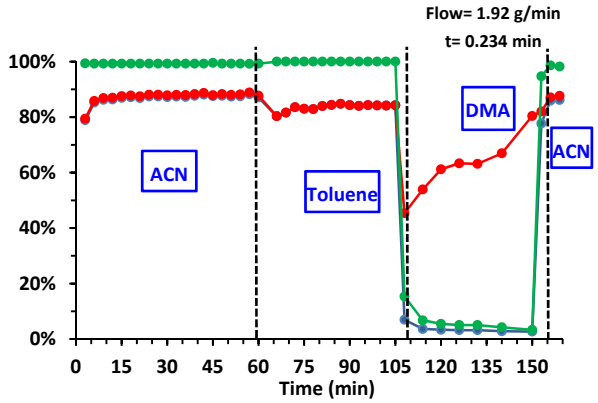

Figure 9. Effect of solvent over α-PO conversion and CA yield and selectivity in fixed bed. Reaction conditions: 450 mg of catalyst (0.2<particle size<0.4mm), 2 mmol of α-PO per 0.48 mL of solvent, contact time from 0.229 min, i.e. total flow from 5.28 mL/min. ● CA yield, ● CA selectivity, ● α-PO conversion.

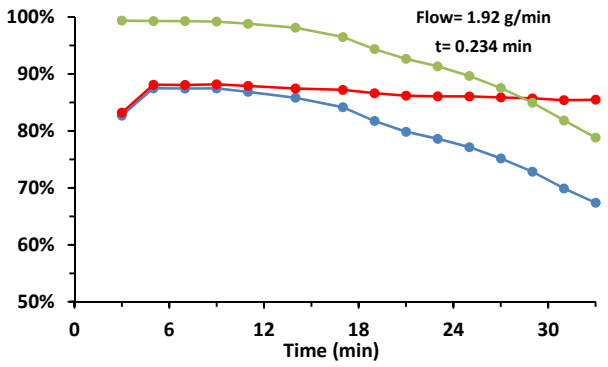

Figure 10. Catalytic performance of Ti-Beta-F for α-PO conversion and CA yield and selectivity in fixed bed. Reaction conditions: Fixed bed, 450 mg of catalyst (0.2<particle size<0.4mm), 2 mmol of α-PO per 0.48 mL of solvent, contact time from 0.229 min, i.e. total flow from 5.28 mL/min. ● CA yield, ● CA selectivity, ● α-PO conversion.

Please do not adjust margins

Please do not adjust margins

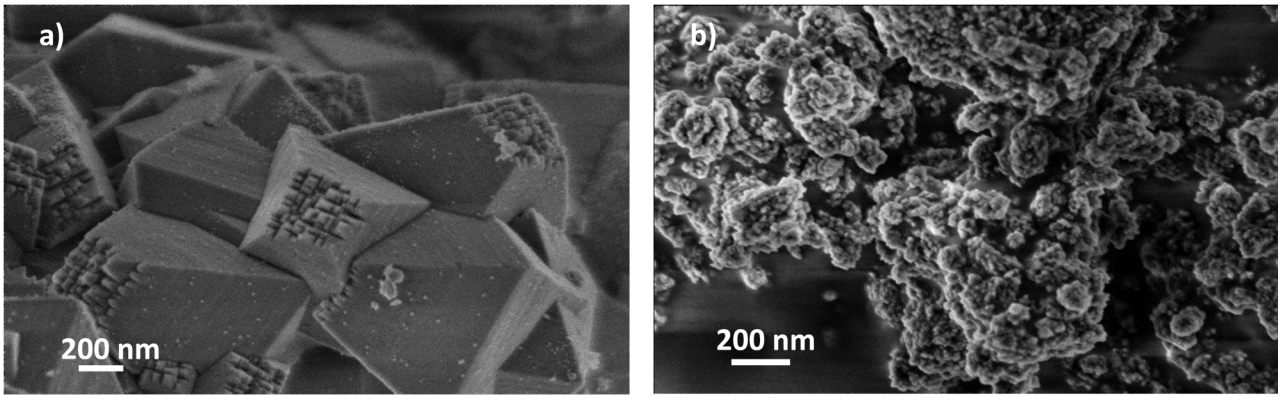

Figure 11. HRFESEM images of Ti-Beta-F and Ti-Beta-PS.

reversible process, since when new ACN solution of α-PO was fed, the catalyst recovered its catalytic properties. The results in fixed bed were in agreement with those obtained in sealed vial under microwave. Moreover the excellent catalytic behaviour of the post synthetic material was clear as well as its stability. Indeed, when the study of temperature was performed 673g of α-PO were reacted over 0.45g without observing catalyst deactivation. These results allowed a CA production of 225 $g/g_{cat}/h$, using α-PO in acetonitrile solution of 2.39 mol/L and achieving 88% CA selectivity at maximum α-PO conversion. These results in terms of selectivity are comparable to the best published results in the presence of $ZnBr_2$ [4] or MOF [34] and slightly lower than in the presence of Ti-MCM22 [3]. Nevertheless, taking into account CA production, amount of catalyst, α-PO concentration and readily availability of the catalysts and cost, results reported in this work offer new opportunities to the development of greener industrial applications. Moreover if the catalytic data are compared to ones reported in 1998 by van Bekkum and co-workers [2] in flow using Ti-beta samples, the CA production is 490 times higher.

Finally the catalytic behaviour of conventional Ti-Beta sample prepared in fluoride media (Ti-Beta-F) in fixed bed was studied (Figure 10). A rapid deactivation of the Ti-Beta-F was observed after 14 min of time on stream with a constant decay of α-PO conversion with time. The catalytic behaviour of Ti-Beta-F was very different to Ti-Beta-PS-HT-Na(0.1%) plotted in Figure 8 and Figure 9 where the catalyst exhibited high catalytic performance and stability. Moreover, Ti-Beta-PS-HT-Na(0.1%) presented ability to recover its catalytic properties after deactivation due to the use of inadequate temperature or solvent. This result was attributed to the morphology and size of the Ti-Beta-F particle. Indeed, the synthesis in fluoride media was characterised by long time of synthesis and the production of particles with large diameter. While the Ti-Beta-PS zeolite sample issued of two synthesis steps, the first of dealumination in acid media of Al-Beta and the second of ball-milling to incorporate Ti, was expected to have smaller particle size due to acid treatment and friction effects. The difference in particle sizes was confirmed through high resolution field emission scanning electron microscopy. Images of Figure 11 illustrate the differences in the particles sizes of both samples close to 500 and 15 nm for Ti-Beta-F and Ti-Beta-PS, respectively.

3. Conclusions

Post-synthesis Ti-Beta zeolite from readily available Al-Beta was prepared via ball-milling. The catalytic performance of the titanosilicate materials was successfully matched to maximize the CA selectivity through controlled hydrothermal Na and Li cation exchange and calcination step. The different population of open and closed Lewis active sites and weak Brønsted acid sites were characterized by IR of CD_3CN adsorption. It was shown that the presence of alkali metal allowed not only to passivate the weak Brønsted acidity of SiO-H adjacent to Ti-atoms but also to induce a weakening in the Ti-Lewis acidity strength. Then, the post-synthesised modified samples exhibited excellent catalytic performance for the α-PO isomerization. Moreover, the optimization of the parameters of reaction led to develop a greener and sustainable process in both batch and flow reactor. From different point of views such as the preparation of readily, highly active, selective and stable catalyst, throughput, sustainability and cost, herein we considered that the selective solid catalysed α-PO isomerization was reported with excellent results and opportunities.

Conflicts of interest

There are no conflicts to declare.

Acknowledgements

The authors are grateful for financial support from the Spanish Government by MAT2017-82288-C2-1-P and Severo Ochoa Excellence Program SEV-2016-0683. Mr. Pablo Ramos contribution to the experimental work is also gratefully acknowledged.

Notes and references

1 M. Stekrova, N. Kumar, A. Aho, I. Sinev, W. Grünert, J. Dahl, Jorma Roine, S. S. Arzumanov, P. Mäki-Arvela, D. Yu. M., *Appl. Catal. A: General, 2014,* **470**, 162.

2 P. J. Kunkeler, J. C. van der Waal, J. Bremmer, B. J. Zuurdeeg, R. Downing and H. van Bekkum, *Catal. Lett.,* 1998, **53**, 135.

This journal is © The Royal Society of Chemistry 20xx

Please do not adjust margins

Please do not adjust margins

3 M. Pitínová-Štekrová, P. Eliášová, T. Weissenberger, M. Shamzhy, Z. Musilová and J. Čejka, *Catal. Sci. Technol*., 2018, **8**, 4690.
4 B. Arbushow, *Chem. Ber*., 1935, **68**, 1430.
5 K. Arata and K. Tanabe, *Chem. Lett*., 1979, **8**, 1017.
6 J. Kaminska, M. A. Schwegler, A. J. Hoefnagel and H. van Bekkum, *Recl. Trav. Chim. Pays-Bas*, 1992, **111**, 432.
7 D. R. C. Huybrechts, L. De Bruycker and P. A. Jacobs, *Nature*, 1990, **345**, 240.
8 C. Ferrini and H. W. Kouwenhoven, *New Developments in Selective Oxidation, ed. G. Centi and F. Trifiro, Elsevier, Amsterdam*, 1990, 53.
9 M. A. Camblor, A. Corma and J. Perez-Pariente, SP Pat. 9 101 798, 1991.
10 M. A. Camblor, M. Costantini, A. Corma, L. Gilbert, P. Esteve, A. Martinez and S. Valencia, *Chem. Commun*., 1996, **11**, 1339.
11 T. Blasco, M. A. Camblor, A. Corma, P. Esteve, A. Martinez, C. Prieto and S. Valencia, *Chem. Commun*., 1996, **20**, 2367.
12 P. Li, G. Liu, H. Wu, Y. Liu, J. Jiang, P. Wu, *J. Phys. Chem. C*, 2011, **115**, 3663.
13 J. Dijkmans, D. Gabriels, M. Dusselier, F. De Clippel, P. Vanelderen, K. Houthoofd, A. Malfliet, Y. Pontikes, B. F. Sels, *Green Chem*., 2013, **15**, 2777.
14 C. Hammond, S. Conrad, I. Hermans, *Angew. Chem., Int. Ed.,* 2012, **51**, 11736.
15 P. Wolf, C. Hammond, S. Conrad and I. Hermans, *Dalton Trans*., 2014, **43**, 4514.
16 C. Hammond, S. Conrad, I. Hermans, *Angew. Chem. Int. Edit*., 2012, **51**, 11736.
17 J. Dijkmans, D. Gabriels, M. Dusselier, F. de Clippel, P. Vanelderen, K. Houthoofd, A. Malfliet, Y. Pontikes, B.F. Sels, *Green Chem*., 2013, **15**, 2777.
18 S. Tolborg, I. Sadaba, C. M. Osmundsen, P. Fristrup, M. S. Holm, and T. Esben, *ChemSusChem*, 2015, **8**, 613.
19 M. A Camblor, A. Corma, J. Perez-Pariente, *Zeolites,* 1993, **13**, 82.
20 N. Garcia Vargas, S. Stevenson, D. F. Shantz, *Microporous Mesoporous Mater*., 2012, **152**, 37.
21 T. Tatsumi, K. A. Koyano, Y. Shimizu, *Appl. Catal. A*, 2000, **200**, 125.
22 C. B. Khouw, M. E. Davis, *J. Catal*., *1995*, **151**, 77.
23 Y. Kuwahara, K. Nishizawa, T. Nakajima, T. Kamegawa, K. Mori, H. Yamashita, *J. Am. Chem. Soc*., 2011, **133**, 12462.
24 E. Taarning, S. Saravanamurugan, H. M. Spangsberg, J. Xiong, R. M. West, and C. H. Christensen, *ChemSusChem*, 2009, **2**, 625.
25 R. Bermejo-Deval, M. Orazov, R. Gounder, S. j. Hwang, and M. E. Davis, *ACS Catal*., 2014, **4**, 2288.
26 T. Blasco, M. A. Camblor, A. Corma, P. Esteve, J. M. Guil, A. Martınez, J. A. Perdigon-Melon, and S. Valencia*, J. Phys. Chem. B*, 1998, **102**, 75.
27 R. K. Iler, *The Chemistry of Silica; Wiley: New York*, 1979.
28 M. J. Cordon, J. W. Harris, J. C. Vega-Vila, J. S. Bates, S. Kaur, M. Gupta, M. E. Witzke, E. C. Wegener, J. T. Miller, D. W. Flaherty, D. D. Hibbitts, and R. Gounder, *J. Am. Chem. Soc*., 2018, **140**, 14244.
29 M. Boronat, P. Concepción, A. Corma, M. Renz, S. Valencia, *J. Catal*., 2005, **234**, 111.
30 D. Gleeson, G. Sankar, C.R.A. Catlow, J.M. Thomas, G. Spano, S. Bordiga, A. Zecchina, C. Lamberti, *Phys. Chem. Chem. Phys.,* 2000, **2**, 4812.
31 R. Otomo, R. Kosugi, Y. Kamiya, T. Tatsumi and T. Yokoi, *Catal. Sci. Technol*., 2016, **6**, 2787.
32 S. Imamura, T. Nakai, H. Kanai and T. Ito, *J. Chem. Soc.,Faraday Trans*., 1995, **91**, 1261.
33 G. Yang, L. Zhou, *Scientific Reports,* 2017, **7**, 16113.
34 L. Alaerts, E. Séguin, H. Poelman, F. Thibault-Starzyk, P. A. Jacobs and D. E. De Vos, *Chem. Eur. J.*, 2006, **12**, 7353.

Please do not adjust margins